Dilepton Backward Rapidity Distributions

M. B. Gay Ducati
beatriz.gay@ufrgs.br

High Energy Phenomenology Group

Instituto de Física

Universidade Federal do Rio Grande do Sul

Porto Alegre, Brazil

GFPAE - UFRGS

http://www.if.ufrgs.br/gfpae

Talk based on works Phys. Lett. B 636, 46 (2006) and hep-ph/0607247.

Outline

- Motivation;
- High Density System
- Forward rapidities;
  - Color Glass Condensate;
  - Saturation effects;
  - p_T and rapidity distributions;
  - Cronin data on hadron production at forward rapidities.
- Backward rapidities;
  - Dipole approach;
  - nuclear effects at small and large Bjorken x;
  - p_T and rapidity distributions;
  - Cronin data on hadron production at backward rapidities.
- Conclusions.

Motivation

- Dilepton $\Rightarrow$ Clean probe (eletromagnetic interactions);
- Forward rapidities:
  - RHIC and LHC experiments are characterized by a high density of gluons in the nucleus;
  - Those interactions can be described by dense condensates (Color Glass Condensates);
  - Search for signatures of the CGC description of the saturated regime;
  - Cronin peak suppression at forward rapidities for hadrons $\Rightarrow$ Initial/Final state effect?
  - Dilepton $\Rightarrow$ presenting the same suppression (Cronin peak suppression for hadrons $\Rightarrow$ Initial state effect)
- Backward rapidites:
  - Nucleus at large Bjorken x;
  - Information about large x nuclear effects;
  - Pronounced Cronin peak at backward rapidities for hadrons $\Rightarrow$ Initial/Final state effect?
  - Dilepton $\Rightarrow$ which is the behavior at backward??

Partonic System Evolution

- Parton at large Bjorken $x \Rightarrow$ Valence quarks.
- Increasing energy $\Rightarrow$ Sea quarks.
- New partons are emitted.
- Emission probability $\propto \alpha_s \ln\left(\frac{1}{x}\right)$.
- DGLAP and BFKL evolution (only emission diagrams).
- At small x region (high energy limit).
- Density of partons increases.
- Large occupation number (partons eventually overlap).
- Recombination processes (GLR, AGL, BK, JIMWLK).

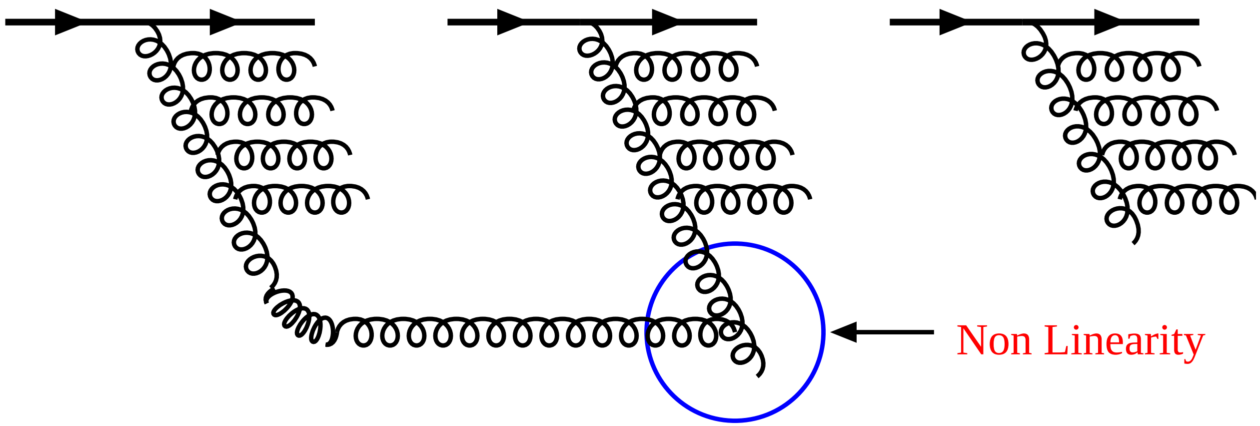

- Gluon dominance at small x.

Partonic System Evolution

- DGLAP and BFKL
- Consider only emission diagrams
- DGLAP $\longrightarrow$ evolution in Q^2 ($\longrightarrow$ diluted system)
- BFKL $\longrightarrow$ evolution in x. ($\longrightarrow$ saturation)
- Saturation $\longrightarrow$ overlap in phase-space (small x and low Q^2).

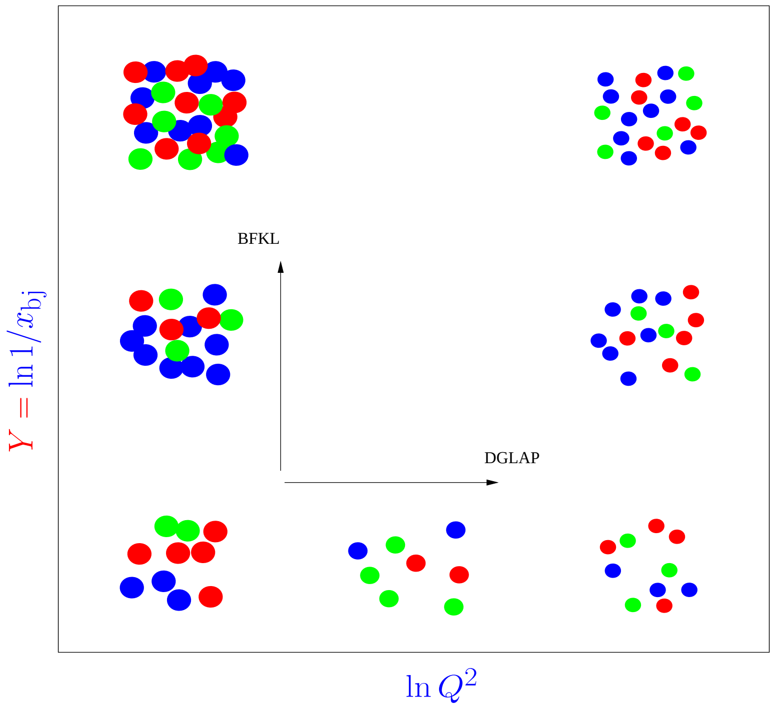

- High density system picture

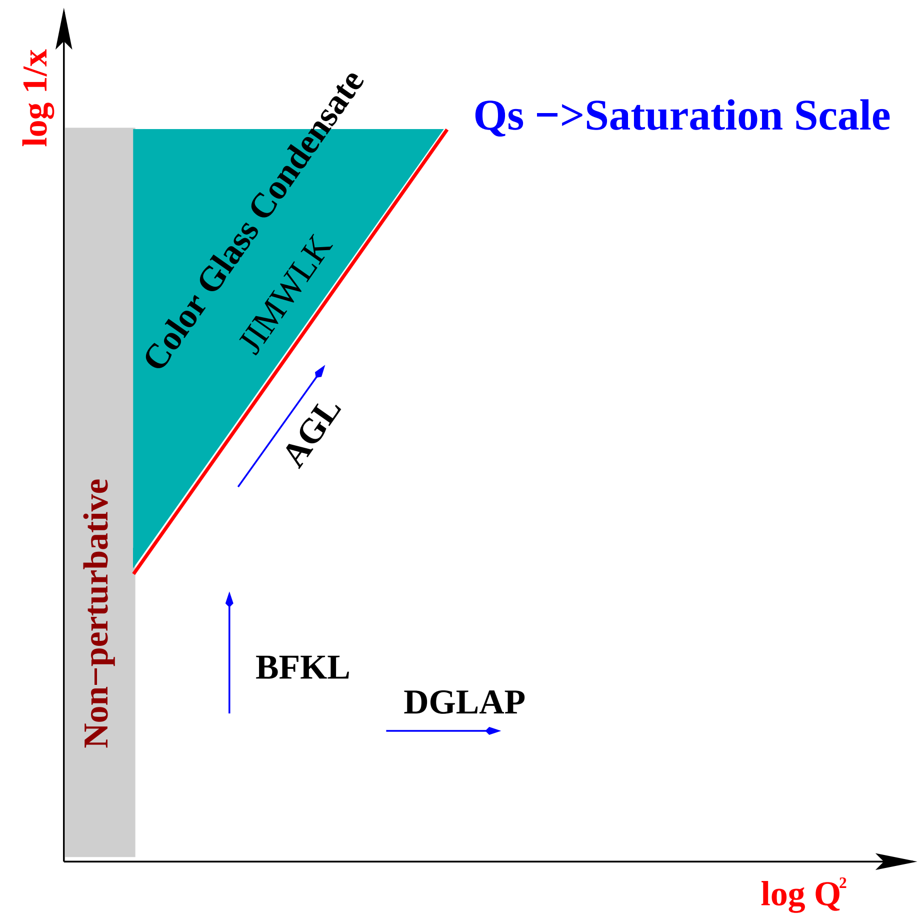

Evolution Equations

- **Linear evolution**
  - DGLAP ($\sim$1977) evolve quark and gluon distributions in Q^2.

$$\frac{dg(x,Q^2)}{d\ln Q^2} = \frac{\alpha_s(Q^2)}{2\pi}\int_x^1 \frac{dy}{y}\left[P_{gq}\left(\frac{x}{y}\right) q_i^S(y,Q^2) + P_{gg}\left(\frac{x}{y}\right) g(y,Q^2)\right],$$

(Dokshitzer, Gribov, Lipatov, Altarelli, Parisi)

  - BFKL ($\sim$1977) evolve non-integated gluon distribution in x.

$$\frac{\partial\phi(x,k_\perp^2)}{\partial\ln(1/x)} = \frac{3\alpha_s}{\pi}k_\perp^2\int_0^\infty \frac{dk_\perp'^2}{k_\perp'^2}\left\{\frac{\phi(x,k_\perp'^2)+\phi(x,k_\perp^2)}{|k_\perp'^2-k_\perp^2|} + \frac{\phi(x,k_\perp^2)}{\sqrt{4k_\perp'^4+k^4}}\right\},$$

(Balitsky, Fadin, Kuraev, Lipatov)

- **Non-linear evolution**
  - GLR (1983) evolve $xg(x,Q^2)$ in x and Q^2.

$$\frac{\partial^2 xg(x,Q^2)}{\partial\ln Q^2\partial\ln 1/x} = \frac{\alpha_s N_c}{\pi}xg(x,Q^2) - \frac{\alpha_s^2\gamma}{Q^2R^2}[xg(x,Q^2)]^2$$

(Gribov-Levin-Ryskin)

  - AGL (1997) evolve $\kappa_G(x,Q^2) = \frac{N_c\alpha_s\pi}{2Q^2R^2}xg(x,Q^2)$ in x and Q^2.

$$\frac{\partial^2\kappa_G(x,Q^2)}{\partial(\ln 1/x)\partial(\ln Q^2)} + \frac{\partial\kappa_G(x,Q^2)}{\partial(\ln 1/x)} = \frac{N_c\alpha_s}{\pi}[C + \ln(\kappa_G) + E_1(\kappa_G)]$$

(Ayala-MBGD-Levin)

  - BK (1996-1999) evolve the the dipole density (N) in x.

$$\frac{\partial^2 N(\vec{x}_{01},\vec{b}_0,Y)}{\partial Y\partial\ln(1/x_{01}^2\Lambda_{QCD}^2)} = \frac{\alpha_s C_F}{\pi}[2 - N(\vec{x}_{01},\vec{b}_0,Y)]N(\vec{x}_{01},\vec{b}_0,Y)$$

(Balitsky-1996; Kovchegov-1999)

  - JIMWLK ($\sim$1997-2001) evolve the color charge sources correlation in $\tau = \ln(1/x)$.

$$\frac{\partial W_\tau[\rho]}{\partial\tau} = \frac{1}{2}\int\frac{\delta}{\delta\rho_\tau^a(x_\perp)}\chi_{ab}(x_\perp,y_\perp)[\rho]\frac{\delta}{\delta\rho_\tau^b(y_\perp)}\mathcal{W}_\tau[\rho],$$

(Jalilian-Marian, Kovner, Leonidov, Weigert, Iancu, McLerran)

Color Glass Condensate (CGC)

L. McLerran, R. Venugopalan (1994)

Developped to describe the nucleus at high energy limit.

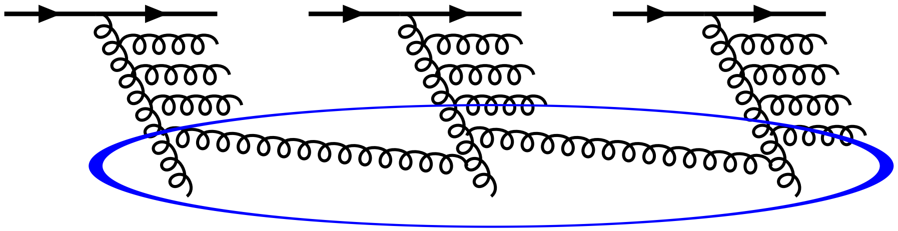

Small x Gluons

- Color $\Rightarrow$ Gluonic field dominance at small x.
- Glass $\Rightarrow$ Internal dynamics evolves slowly compared with the typical interaction scale time.
- Condensate $\Rightarrow$ Dense and saturated gluonic field.

The theory:

- Separation of small x and large x modes.
- Small x modes $\Rightarrow$ large occupation number
  - Described by classical color field $\mathcal{A}^{\mu}$ (CGC)
- Large x modes $\Rightarrow$ acts as sources of the small x modes
  - Described by frozen color sources ρ_a

Color Glass Condensate

- $\mathcal{A}^\mu$ obeys classical Yang-Mills's equations

$$[D_{\mu\nu}, F_a^{\mu\nu}] = \delta^{\mu +}\rho_a(x^-, x_\perp)$$

- $\rho_a(x, x_\perp)$ stochastic variable with zero expectation value.
- average over all ρ_a configurations, with the gauge-invariant weight functional $\mathcal{W}_{\Lambda^+}[\rho_a]$
- $\mathcal{W}_{\Lambda^+}[\rho_a]$ driven by JIMWLK evolution equation.
- $p^+ > \Lambda^+$ fast gluons, $p^+ < \Lambda^+$ soft gluons.
- Observables are calculated by averaging over the sources configurations by means of

$$\langle A_a^i(x^+, \vec{x}) A_b^j(x^+, \vec{y}) ... \rangle_{\Lambda^+} = \int \mathcal{D}_\rho \mathcal{W}_{\Lambda^+}[\rho] \mathcal{A}_a^i(\vec{x}) \mathcal{A}_b^j(\vec{y}).$$

Color Glass Condensate: Phenomenolog

Phenomenology:

- Local Gaussian (can accomodate BFKL evolution and the gluon saturation)

$$\mathcal{W}[x,\rho] = \exp\left\{ -\int dz_\perp \frac{\rho_a(z_\perp)\rho^a(z_\perp)}{2\mu^2(x)} \right\}$$

- Non local Gaussian (Predicted by the mean field asymptotic solution of the JIMWLK evolution equations)

$$\mathcal{W}[x,\rho] = \exp\left\{ -\int dy_\perp dx_\perp \frac{\rho_a(x_\perp)\rho^a(y_\perp)}{2\mu^2(x)} \right\}$$

- $\mu^2(x)$ is the average color charge squared of the valence quarks per unit transverse area and color.
- The color source distribution employed here is a Non-local Gaussian.

Investigating the CGC

- Cronin Effect at forward rapidities.
- Multiple scatterings of the quark with the nucleus environment $\Rightarrow$ transverse momentum broadening.

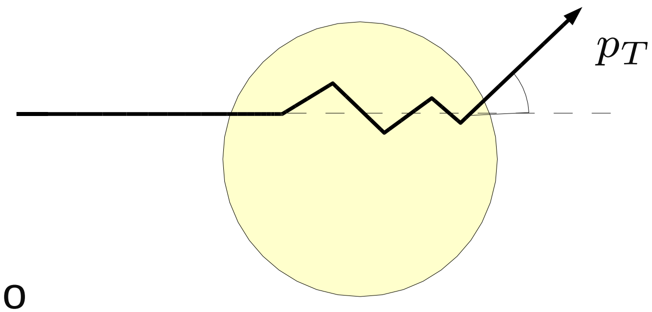

- Nuclear modification ratio

$$R_{dA} = \frac{\frac{d\sigma^{dA\to hX}}{dp_T^2 dy}}{\mathcal{N}_{coll}\frac{d\sigma^{pp\to hX}}{dp_T^2 dy}}$$

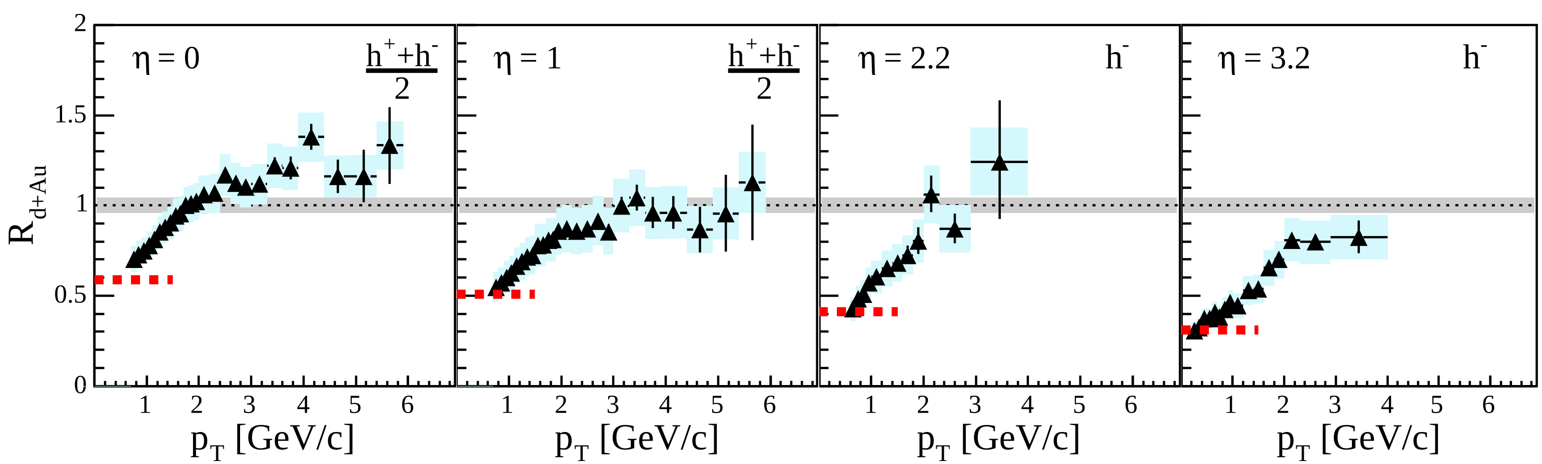

- Central rapidities $\Rightarrow$ Cronin peak
- Suppression of the ratio with the rapidity;

Cronin effect in the CGC approach

charged hadrons

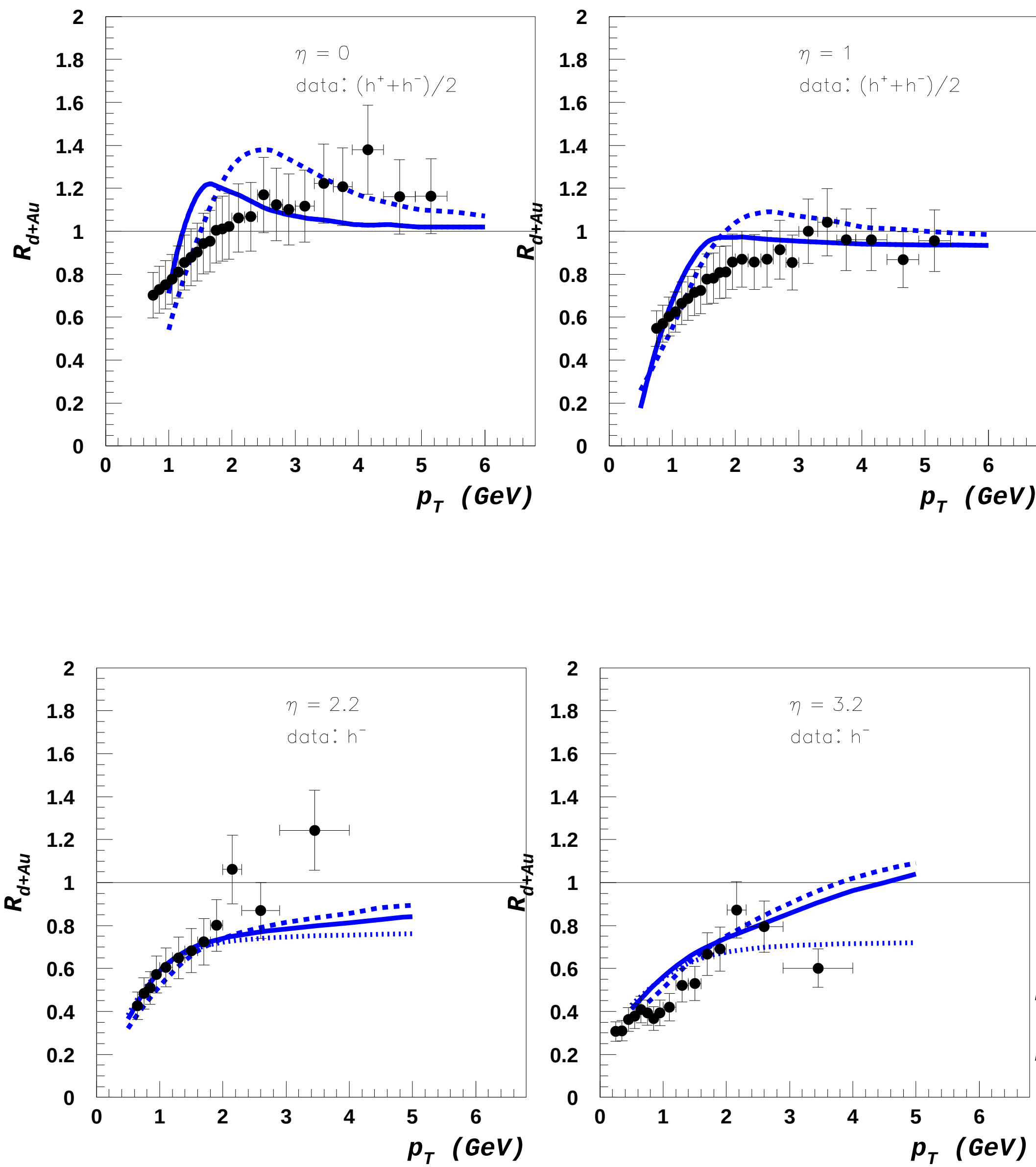

$$R_{dA} = \frac{\frac{d\sigma^{dA \to hX}}{dp_T^2 dy}}{\mathcal{N}_{coll} \frac{d\sigma^{pp \to hX}}{dp_T^2 dy}}$$

- Data from dA collisions at $\sqrt{s} = 200$ GeV.
- BRAHMS data.
- KKP fragmentation function (*Nucl. Phys. B597, 337 (2001)*
- dipole-nucleus forward scattering (CGC)
- Consider valence quarks
- Introduce a function to take into account large x gluon behavior
- Suppression at large rapidities $\Rightarrow$ saturation.

D. Kharzeev, Y. V. Kovchegov, K. Tuchin, Phys. Lett. B **599**, *23 (2004).*

(*J. P. Blaizot, F. Gelis and R. Venugopalan, Nucl. Phys. A* **743**, *13 (2004)*)

Why dilepton production?

Comparing dilepton and hadron productions

- Inclusive hadron production
  - To calculate the p_T and y (rapidity) distributions

$$\frac{d\sigma^{pA\to hX}}{dp_T^2 dy_h} = \frac{d\sigma^{ij\to kX}}{dp_T^2 dy_j} \otimes f_i(y_i, Q_h^2) \otimes f_j(y_j, Q_h^2) \otimes D_{k\to h}(z, Q_h^2)$$

- Needs a fragmentation function $\Rightarrow$ strongly dependent on the final state interactions
- Dilepton production

$$\frac{d\sigma^{pA\to l^+ l_- X}}{dp_T^2 dy} = \frac{d\sigma^{ij\to kX}}{dp_T^2 dy} \otimes f_i(y_i, Q_h^2) \otimes f_j(y_j, Q_h^2).$$

  - Final state interactions are disregarded (eletromagnetic interaction).
  - Cleaner analysis

Dilepton Production in CGC

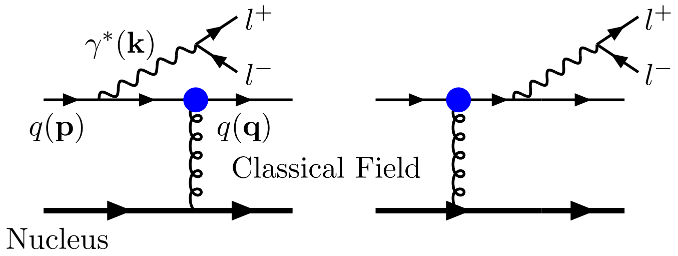

The cross section of dilepton production at forward rapidities can be written as

$$\frac{d\sigma^{pA\to q l^+ l^- X}}{dp_T^2\, dM\, dy} = \frac{4\pi^2}{M} R_A^2 \frac{\alpha_{em}^2}{3\pi} \int \frac{dl_T}{(2\pi)^3} l_T W(p_T, l_T, x_1)\, C(l_T, x_2, A),$$

- $W(p_T, l_T, x_1)$ analytical calculations $\Rightarrow$ wave function in the momentum space.
- $C(l_T, x_2, A)$ color field correlation $\Rightarrow$ interaction of the quark with the condensated gluonic field (Classical field) $\Rightarrow$ information about the CGC.
- Saturation $\Rightarrow$ low p_T

$$C(l_T) \equiv \int d^2x_\perp e^{il_T\cdot x_\perp} \langle U(0)U^\dagger(x_\perp)\rangle_\rho,$$

- $U(x_\perp)$ $\Rightarrow$ interaction of the quark with the color field of the nucleus.
- Here is where the non-local Gaussian is used to obtain $\langle U(0)U^\dagger(x_\perp)\rangle_\rho$

$$\langle U(0)U^\dagger(x_\perp)\rangle = \int \mathcal{D}_\rho \mathcal{W}_{\Lambda^+}[\rho] U(0)U^\dagger(x_\perp).$$

F. Gelis, J.Jalilian-Marian, Phys. Rev. D **66***, 094014 (2002).*

M.A.Betemps, MBGD, Phys. Rev. D **70***, 116005 (2004). Eur. Phys. J. C* **43***, 365 (2005).*

R. Baier, A. H. Mueller and D. Schiff, Nucl. Phys. A **741***, 358 (2004).*

Color Field Correlation

$$C(l_T) \equiv \int d^2x_\perp e^{il_T \cdot x_\perp} \langle U(0)U^\dagger(x_\perp)\rangle_\rho,$$

- Related to the Fourier transform of non-integrated gluon distribution

$$C(l_T) = \frac{1}{\sigma_0}\int d^2 r e^{il_T \cdot r}[\sigma_{dip}(r \to \infty) - \sigma_{dip}(r)],$$

- We have analyzed some models for the correlation function
  - McLerran-Venugopalan
  - GBW
  - Iancu, Itakura and Munier (CGCfit)
- We use McLerran-Venugopalan with non-local Gaussian

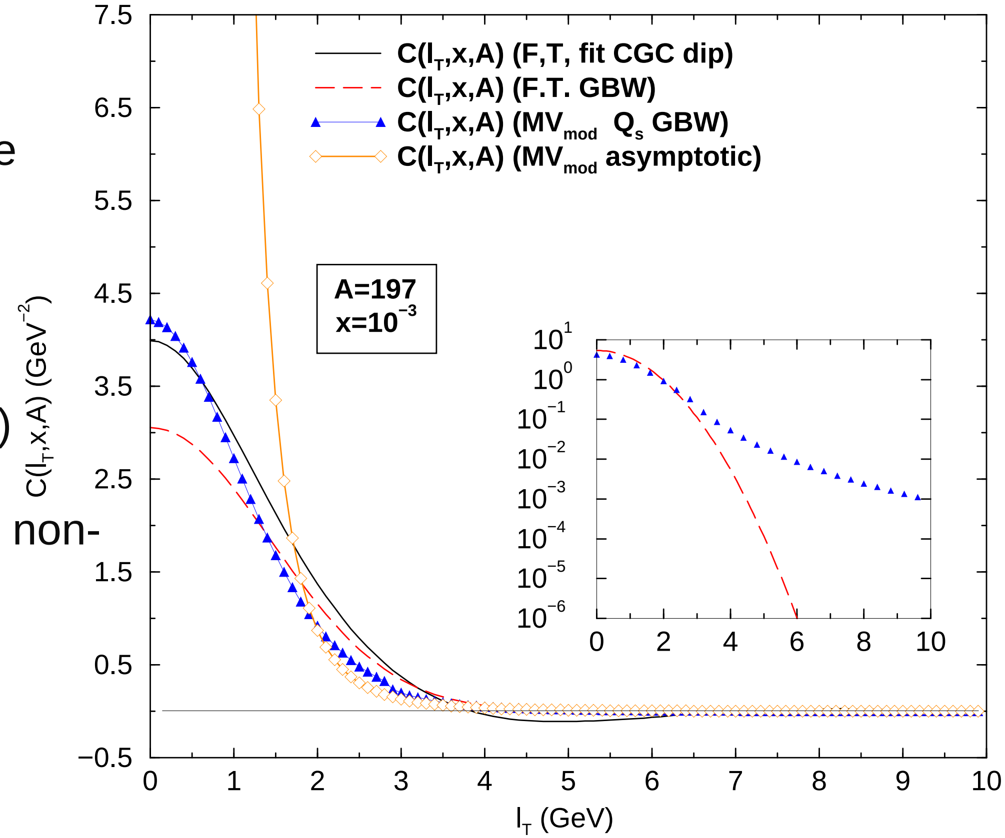

How to investigate the saturation effects considering dilepton production?

Nuclear modification ratio

- Investigating the saturation effects,

$$R_{pA} = \frac{\frac{d\sigma(pA)}{R_A^2 dp_T^2 dy dM}}{A^{1/3} \frac{d\sigma(pp)}{R_p^2 dp_T^2 dy dM}}.$$

- Dilepton mass $M = 6$ GeV.
- RHIC energies $\sqrt{s} = 200$ GeV.
- LHC energies $\sqrt{s} = 8800$ GeV.
- Rapidity and p_T spectra.
- Normalization factor $A^{1/3} \Rightarrow$ cylindrical nucleus $\Rightarrow R_A^2$ in the cross section $\Rightarrow R_A^2 \propto A^{2/3}$.

R_{pA} Forward rapidity and p_T

- RHIC $\sqrt{s} = 200$ GeV

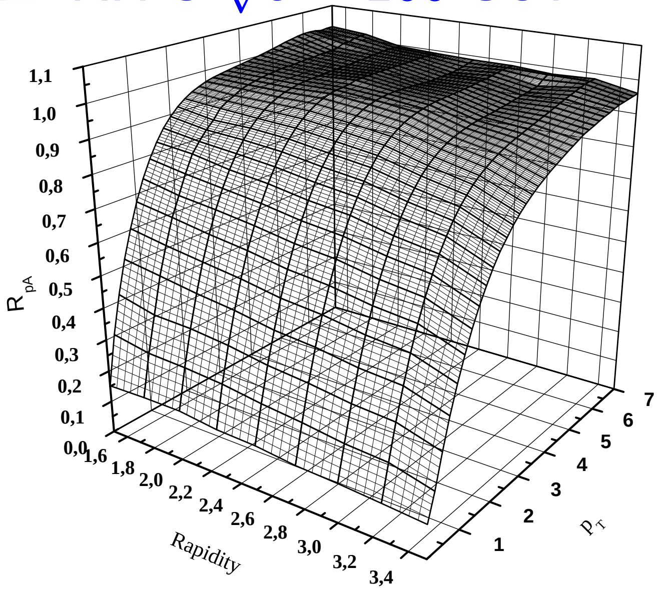

- LHC $\sqrt{s} = 8.8$ TeV

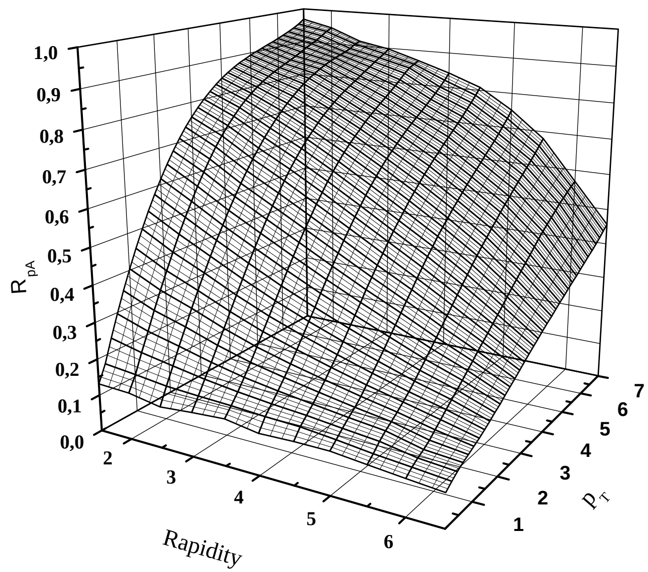

- Lepton pair mass $M = 6$ GeV
- Suppression at small p_T;
- Suppression of the Cronin peak;
- RHIC
  - small effects in the rapidity spectra;
  - Effects are independent of the p_T value;
- LHC
  - Suppression in the rapidity spectra is intensifi ed for large p_T
- Similar behavior of the ratio in p_T at $M = 3$ GeV.

M.A.Betemps, MBGD, Phys. Lett. B, ***636****, 46 (2006).*

Cronin effect at forward rapidities

- BK/BFKL $\Rightarrow$ suppression of the Cronin peak (suppression at small x for all p_T).

charged hadrons

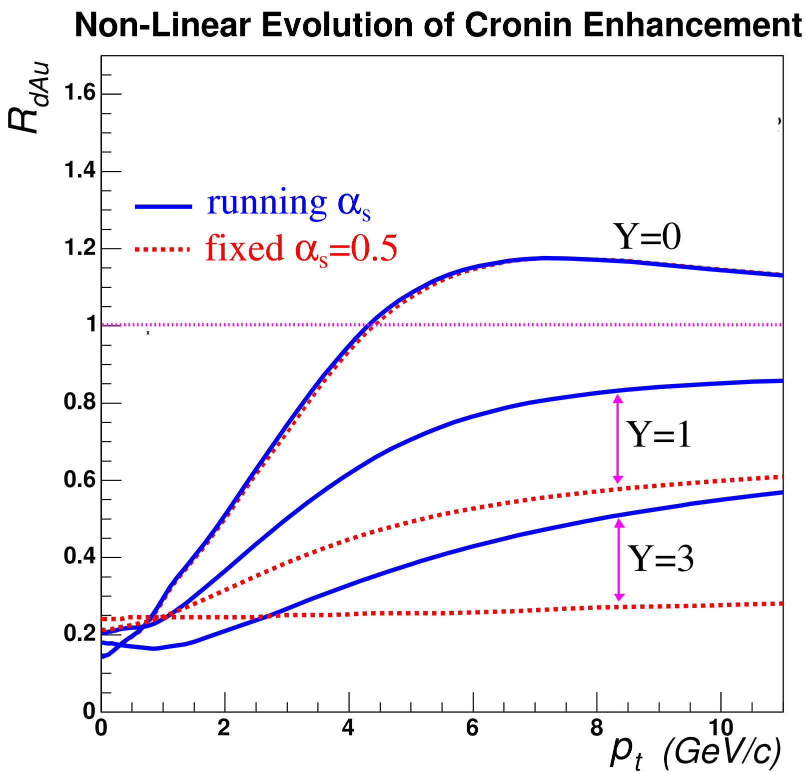

J.V. Albacete et al. Phys. Rev. Lett. **92**, *082001 (2004).*

- Ratio suppression with the rapidity;
- Suppression at forward rapidities $\Rightarrow$ quantum evolution at small x.

Dileptons

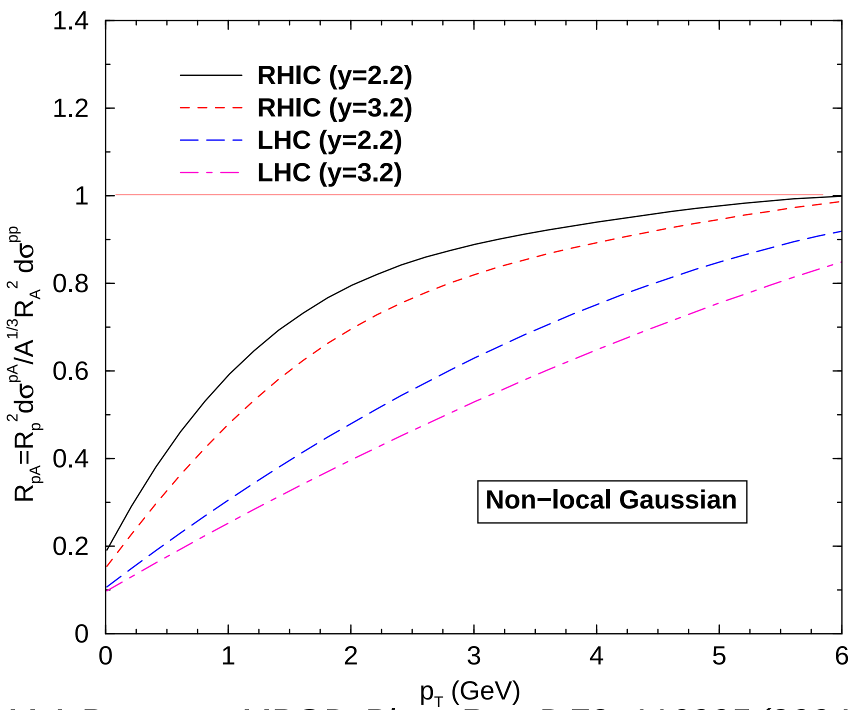

M.A.Betemps, MBGD, Phys. Rev. D **70**, *116005 (2004).*

- Similar behavior of the hadrons;
- Cronin suppression at forward rapidities $\Rightarrow$ Initial state effect;
- Dileptons carry information about the high density QCD system (CGC);

Comparing RHIC and LHC

- Comparing saturation effects at RHIC and LHC.
- Defi ning the ratio,

$$Ratio = \frac{R_{pA}(LHC)}{R_{pA}(RHIC)}$$

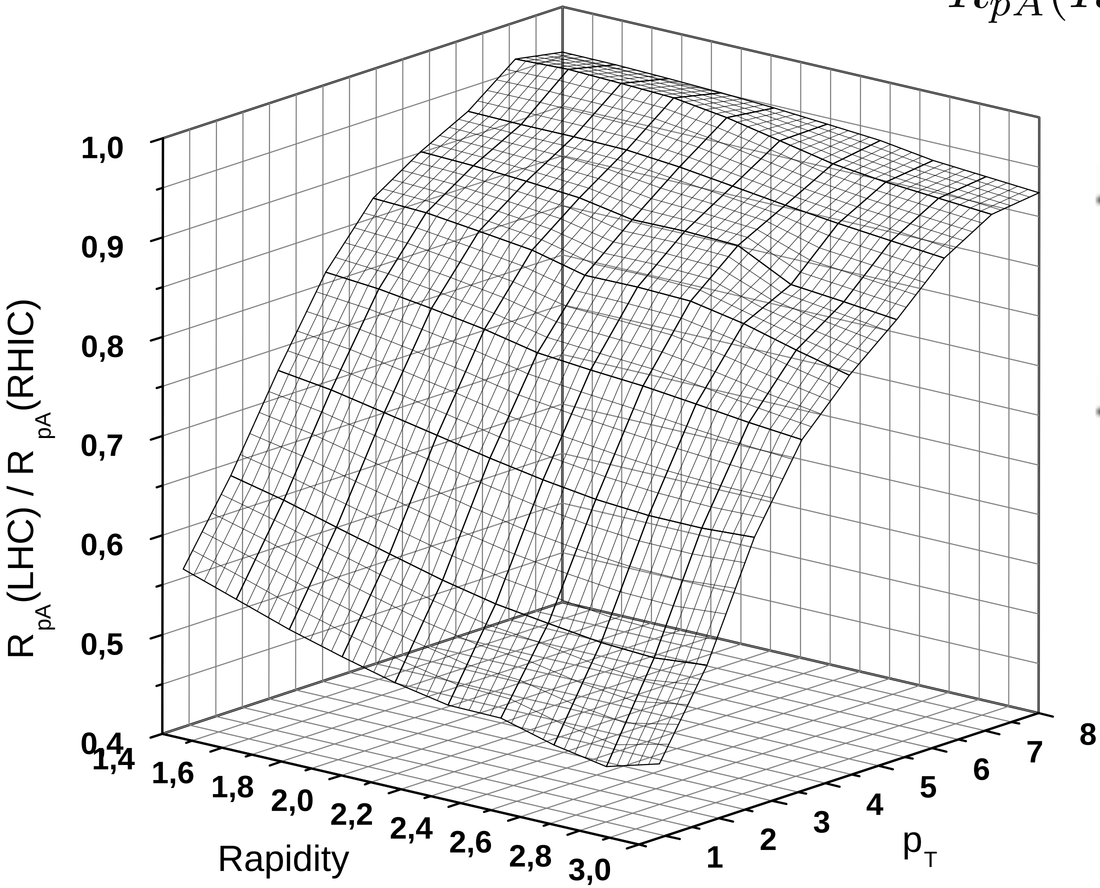

- Small saturation effects in rapidity comparing RHIC and LHC (RHIC range only).
- Large saturation effects at LHC comparing with RHIC in the p_T distribution.

Dilepton at Backward Rapidities

- Dipole picture changing nucleus and proton

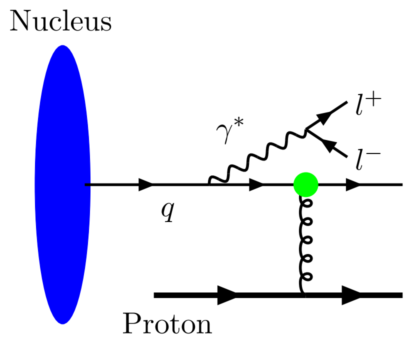

$$\frac{d\sigma^{DY}}{dM^2dyd^2p_T} = \frac{\alpha_{em}^2}{6\pi^3M^2}\int_0^\infty d\rho W(x_2,\rho,p_T)\sigma_{dip}(x_1,\rho),$$

$x_{\binom{1}{2}} = \sqrt{\frac{M^2+p_T^2}{s}}e^{\pm y}$. Large x_2 (nucleus) and small x_1 proton.

$$W(x_2,\rho,p_T) = \int_{x_2}^1 \frac{d\alpha}{\alpha^2}F_2^A(\frac{x_2}{\alpha},M^2)\left\{[m_q^2\alpha^2+2M^2(1-\alpha)^2]\left[\frac{1}{p_T^2+\eta^2}T_1(\rho)-\frac{1}{4\eta}T_2(\rho)\right]\right.$$
$$\left. + [1+(1-\alpha)^2]\left[\frac{\eta p_T}{p_T^2+\eta^2}T_3(\rho)-\frac{1}{2}T_1(\rho)+\frac{\eta}{4}T_2(\rho)\right]\right\},$$

$\alpha \Rightarrow$ momentum fraction of the quark carried by the virtual photon

$$T_1(\rho) = \frac{\rho}{\alpha}J_0(\frac{p_T\rho}{\alpha})K_0(\frac{\eta\rho}{\alpha})$$
$$T_2(\rho) = \frac{\rho^2}{\alpha^2}J_0(\frac{p_T\rho}{\alpha})K_1(\frac{\eta\rho}{\alpha}) \qquad (\eta^2 = (1-\alpha)M^2+\alpha^2m_q^2)$$
$$T_3(\rho) = \frac{\rho}{\alpha}J_1(\frac{p_T\rho}{\alpha})K_1(\frac{\eta\rho}{\alpha}).$$

M.A. Betemps, MBGD, E.G. de Oliveira, hep-ph/0607247.

Coherence length (l_c) at backward

- mean lifetime of fluctuation $|ql^+l^-\rangle$.
- Important quantity controlling $\Rightarrow$ nuclear effects.
- l_c smaller than the target (Fig (a))
  $\Rightarrow$ energy loss in the target (there is no significative energy loss with proton target).

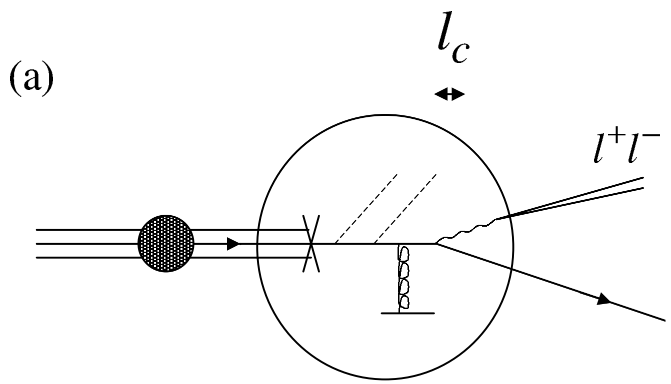

- l_c larger than the target (Fig (b)) $\Rightarrow$ cross section in the factorized form

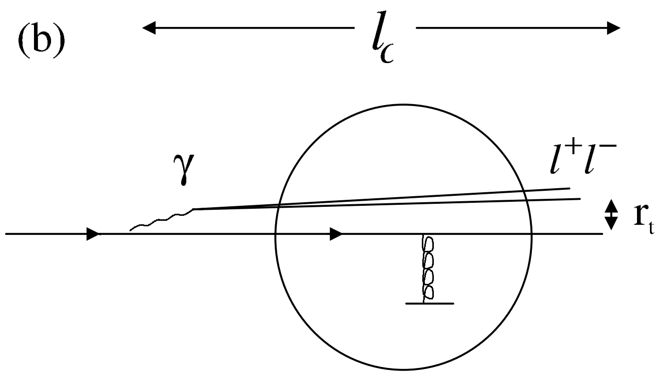

M.B.Johnson, et al. Phys. Rev. Lett. **86**, *4483 (2001).*

l_c at backward (our case - insight for backward)

- Consider here large $l_c \propto \frac{1}{x_1} \Rightarrow x_1$ momentum fraction of the proton target.
- Applicable only at small x_1 (proton).
- Explain the exchange between proton and nucleus in the dipole approach.

Nuclear parton distributions and σ_{dip}

- Eskola, Kolhinen and Salgado (EKS parametrization) *Eur. Phys. J. C* **9**, *61 (1999)*
- D. de Florian and R. Sassot (nDS parametrization) *Phys. Rev. D* **69**, *074028 (2004)*

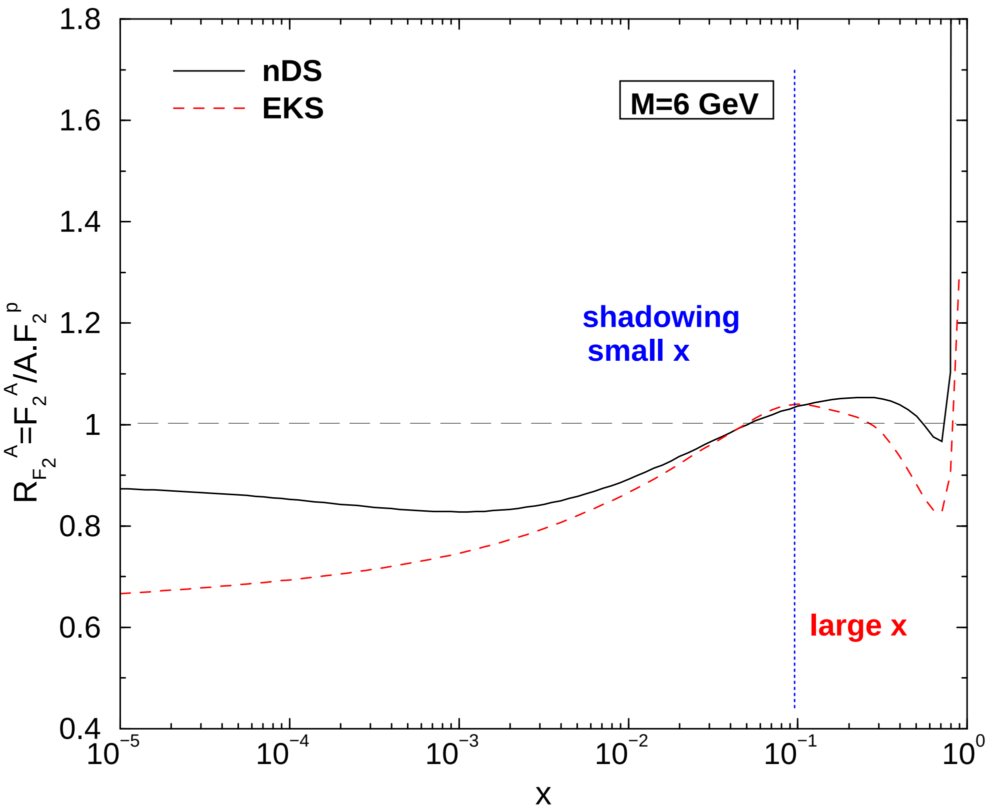

- $\sigma_{dip} \Rightarrow$ GBW dipole cross section $\sigma_{dip}(x,r) = \sigma_0 (1 - \exp\left\{\left(\frac{r^2 Q_0^2}{4(x/x_0)^\lambda}\right)\right\}$
- Fit to the HERA data ($\sigma_0 = 23.03$mb, $x_0 = 3.04 \times 10^{-4}$, $\lambda = 0.288$)

K. Golec-Biernat, M. Wusthoff, Phys. Rev. D **59**, *014017 (1999)*

Nuclear modification ratio

- Investigating effects in the backward region,

$$R_{pA} = \frac{\frac{d\sigma(pA)}{dp_T^2 dy dM}}{A \frac{d\sigma(pp)}{dp_T^2 dy dM}}.$$

- Dilepton mass $M = 6$ GeV.
- RHIC energies $\sqrt{s} = 200$GeV.
- LHC energies $\sqrt{s} = 8800$ GeV.
- Rapidity and p_T spectra.
- Normalization factor $A \Rightarrow$ nucleus confi guration $\rightarrow$ there is no R_A^2 in the cross section.

Backward y and p_T at RHIC (EKS)

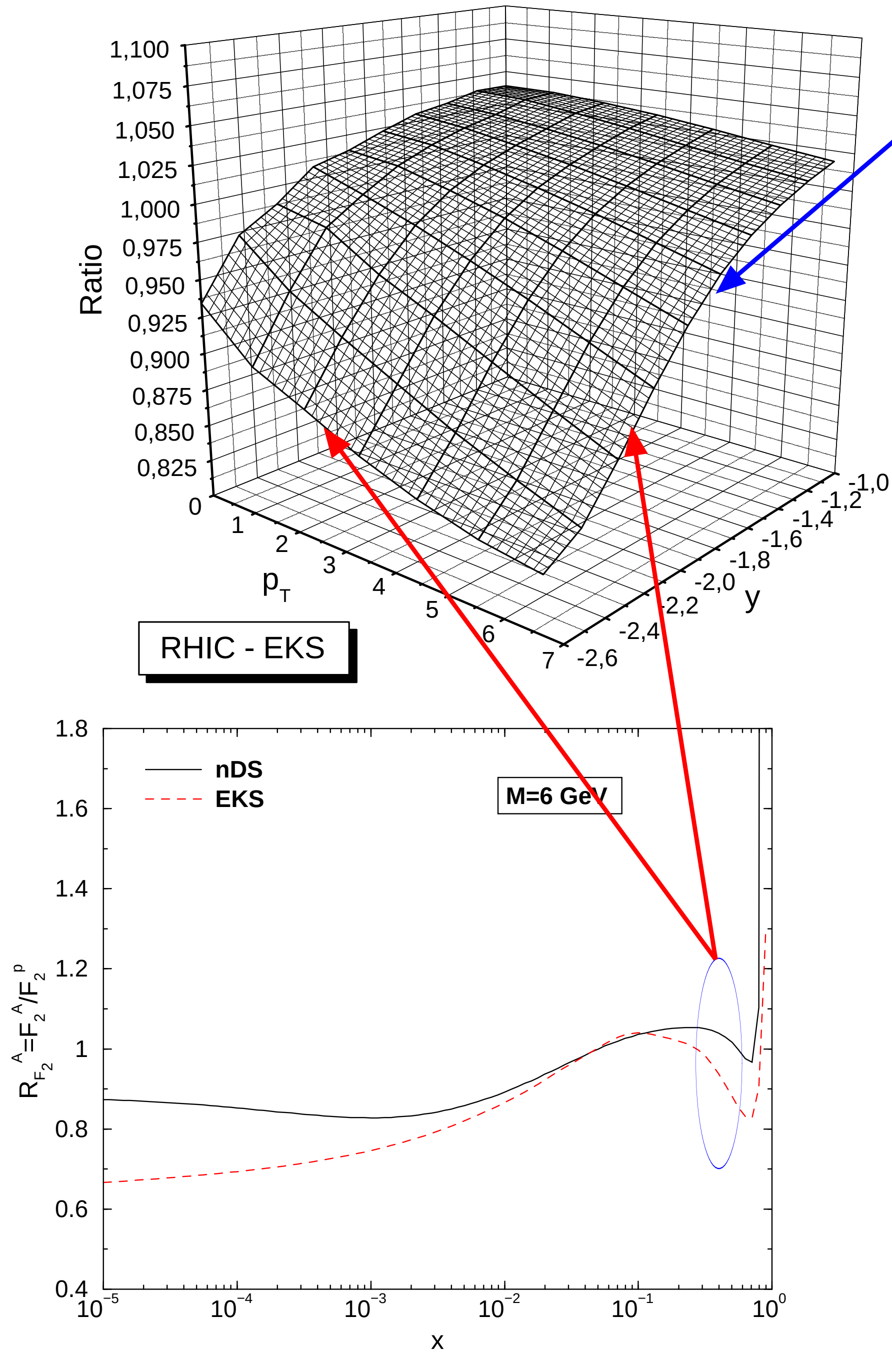

- $0.08 < x_2 < 0.5$.
- Large x nuclear effect;
- lower $y \rightarrow$ large x_2
- Suppression in $y \rightarrow$ large x effect;
- large $p_T \rightarrow$ large x_2;
- Suppression in $p_T \rightarrow$ large x effect $\rightarrow$ less intense;
- Comparison EKS $\times$ nDS (large x effect predictions).

Backward y and p_T at RHIC (nDS)

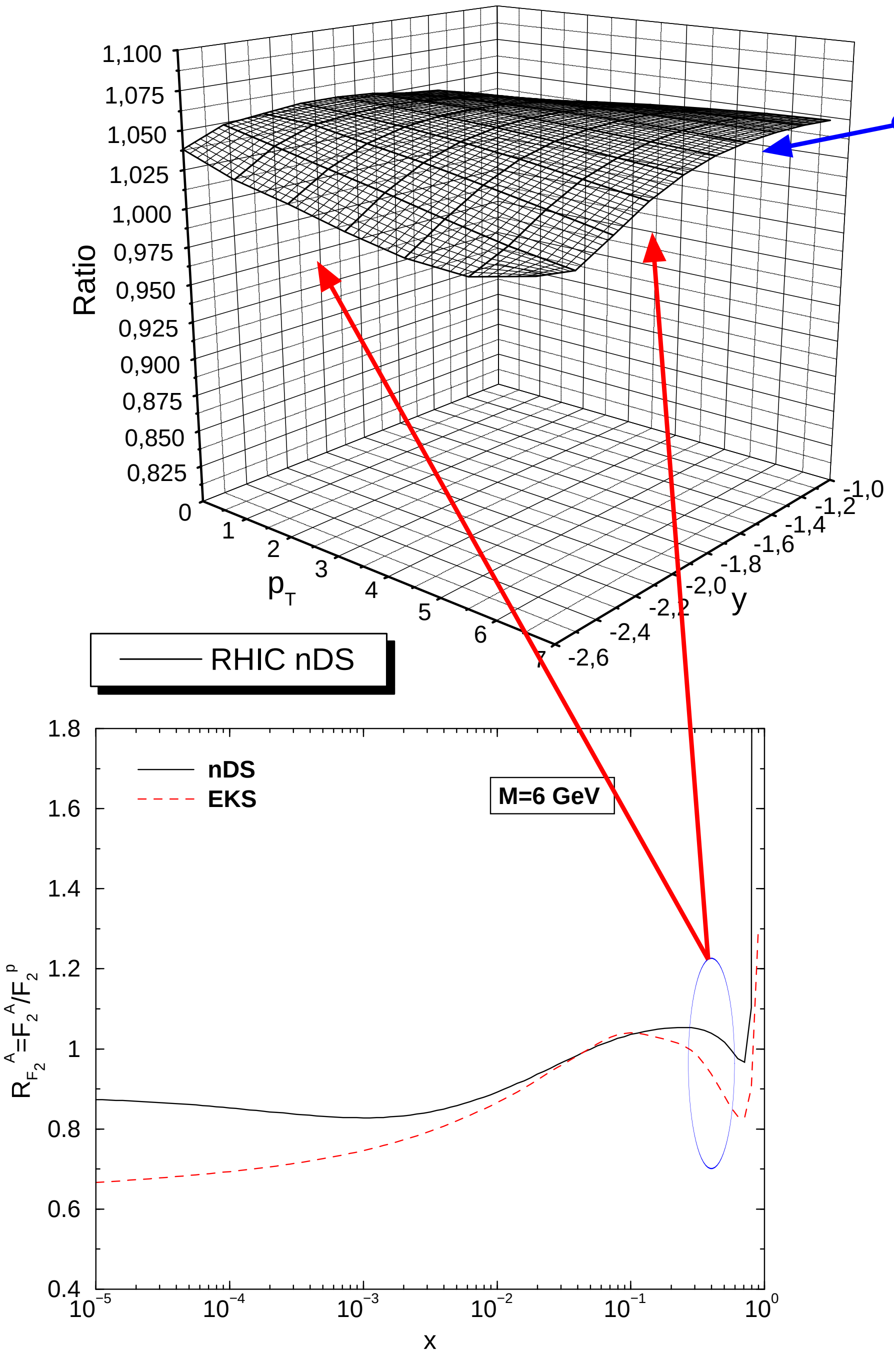

- $0.08 < x_2 < 0.5$.
- Large x nuclear effect;
- lower $y \to$ large x_2
- Suppression in $y \to$ large x effect;
- large $p_T \to$ large x_2;
- Suppression in $p_T \to$ large x effect $\to$ less intense;
- Comparison EKS $\times$ nDS (large x effect predictions).

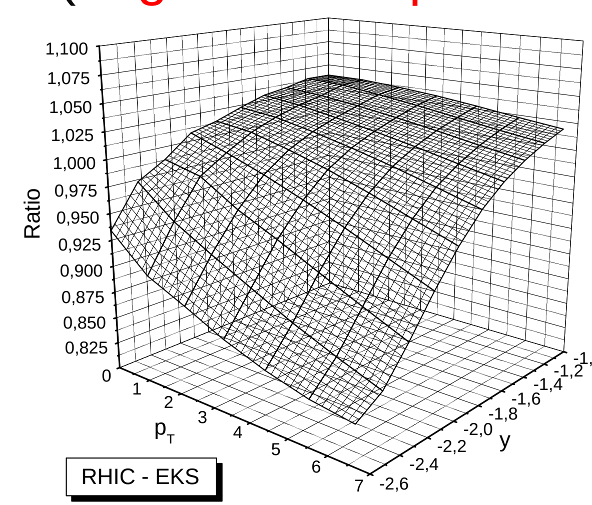

Backward y and p_T at LHC (EKS)

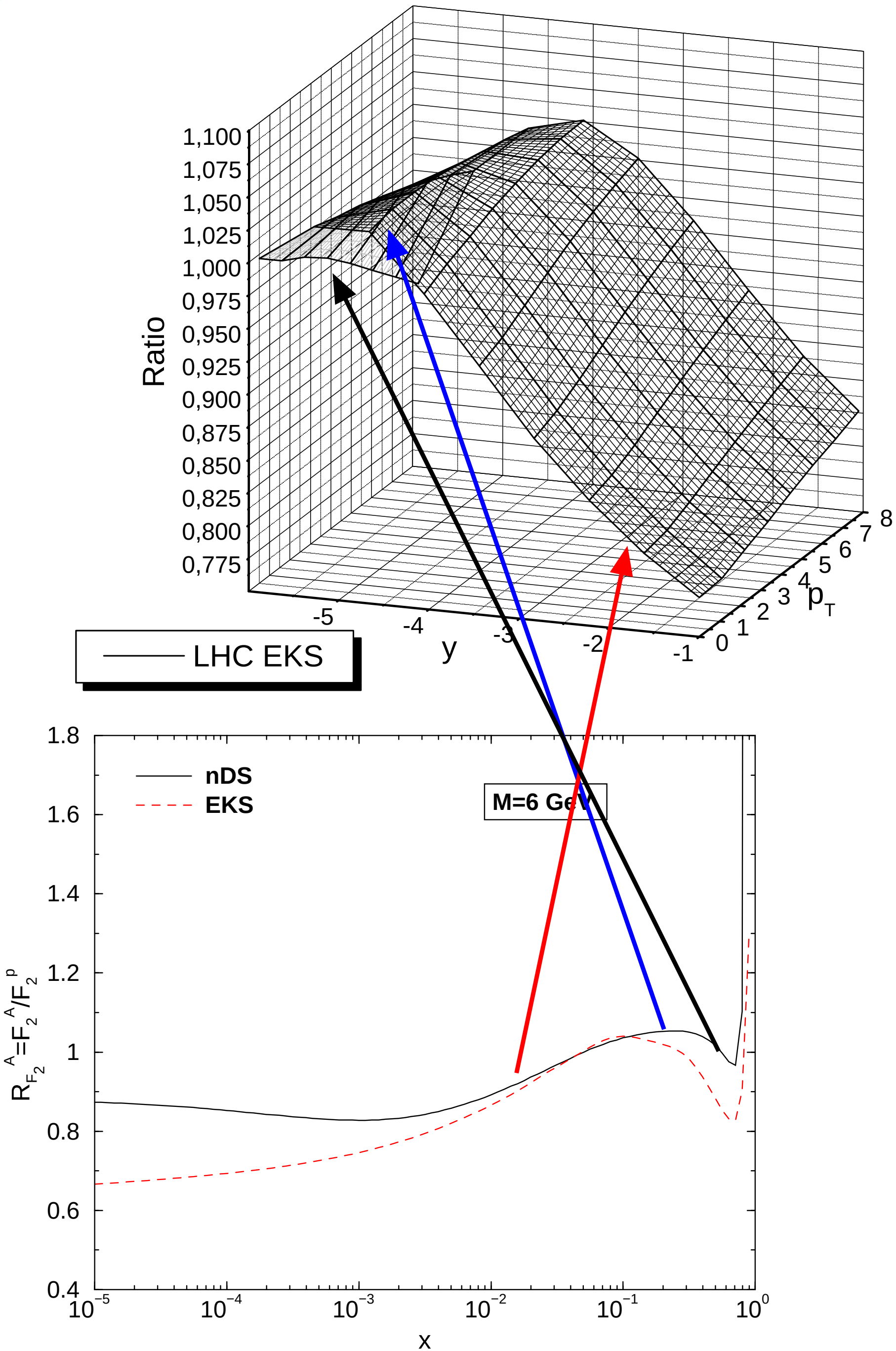

- $0.002 < x_2 < 0.3$.
- antishadowing and shadowing nuclear effects;
- Peak at $y \sim -4.5 \rightarrow$ antishadowing effect;
- Two behaviors with p_T:
  - Suppression in $p_T \rightarrow$ large x effect (very backward);
  - Decreasing with $p_T \rightarrow$ shadowing effect;
- EKS $\times$ nDS (similar behavior)
- Caution with the terminology and interpretation: Nuclear pdf's not pdf's.

Backward y and p_T at LHC (nDS)

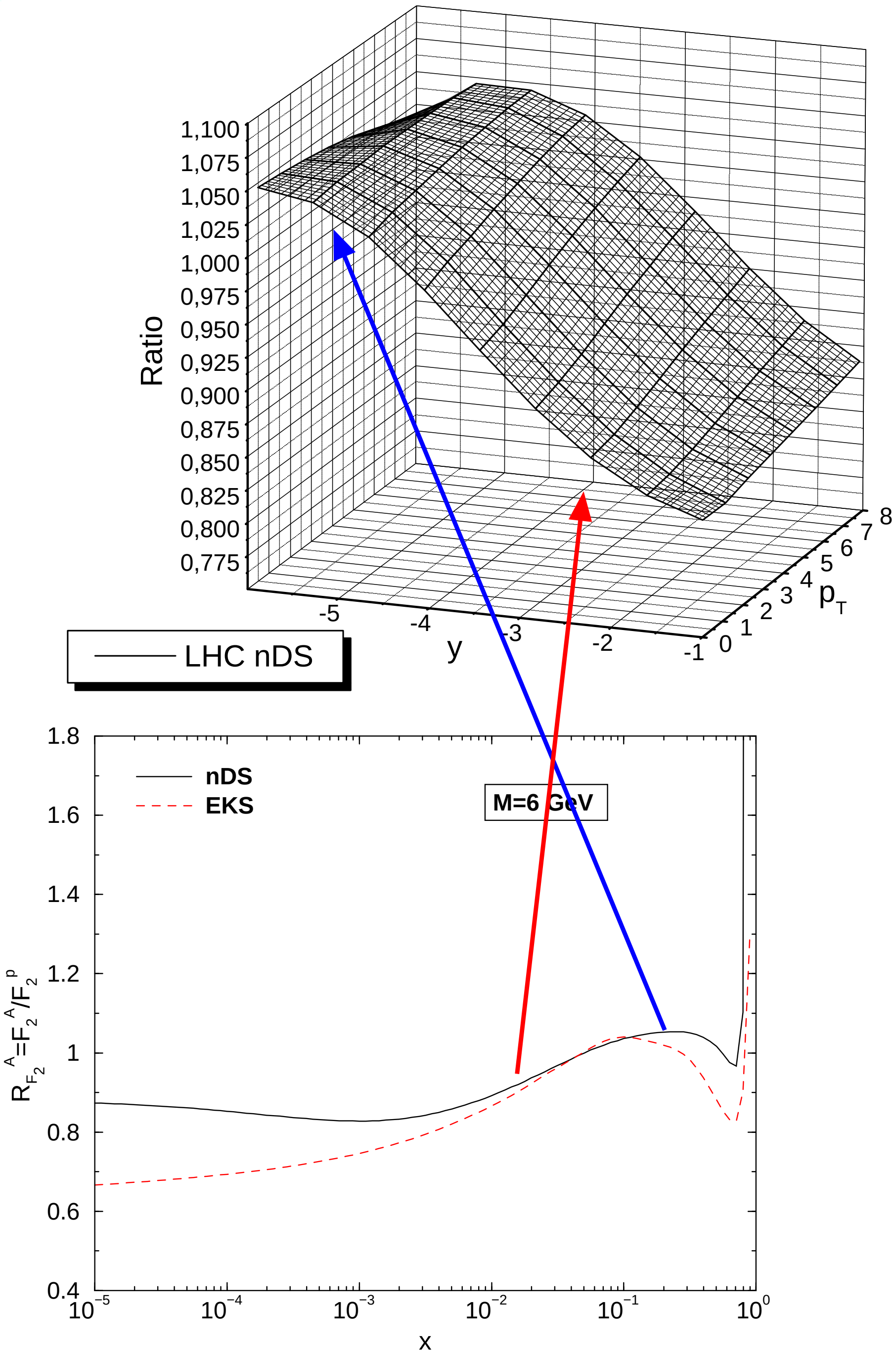

- $0.002 < x_2 < 0.3$.
- antishadowing and shadowing nuclear effects;
- Peak at $y \sim -5 \rightarrow$ antishadowing effect;
- Two behaviors with p_T:
  - Suppression in $p_T \rightarrow$ large x effect (only at very backward);
  - Decreasing with $p_T \rightarrow$ shadowing effect;
- Weak p_T dependence;
- EKS $\times$ nDS (similar behavior)
- Caution with the terminology and interpretation: Nuclear pdf's not pdf's.

Dilepton at backward-forward rapidities

- RHIC energies.

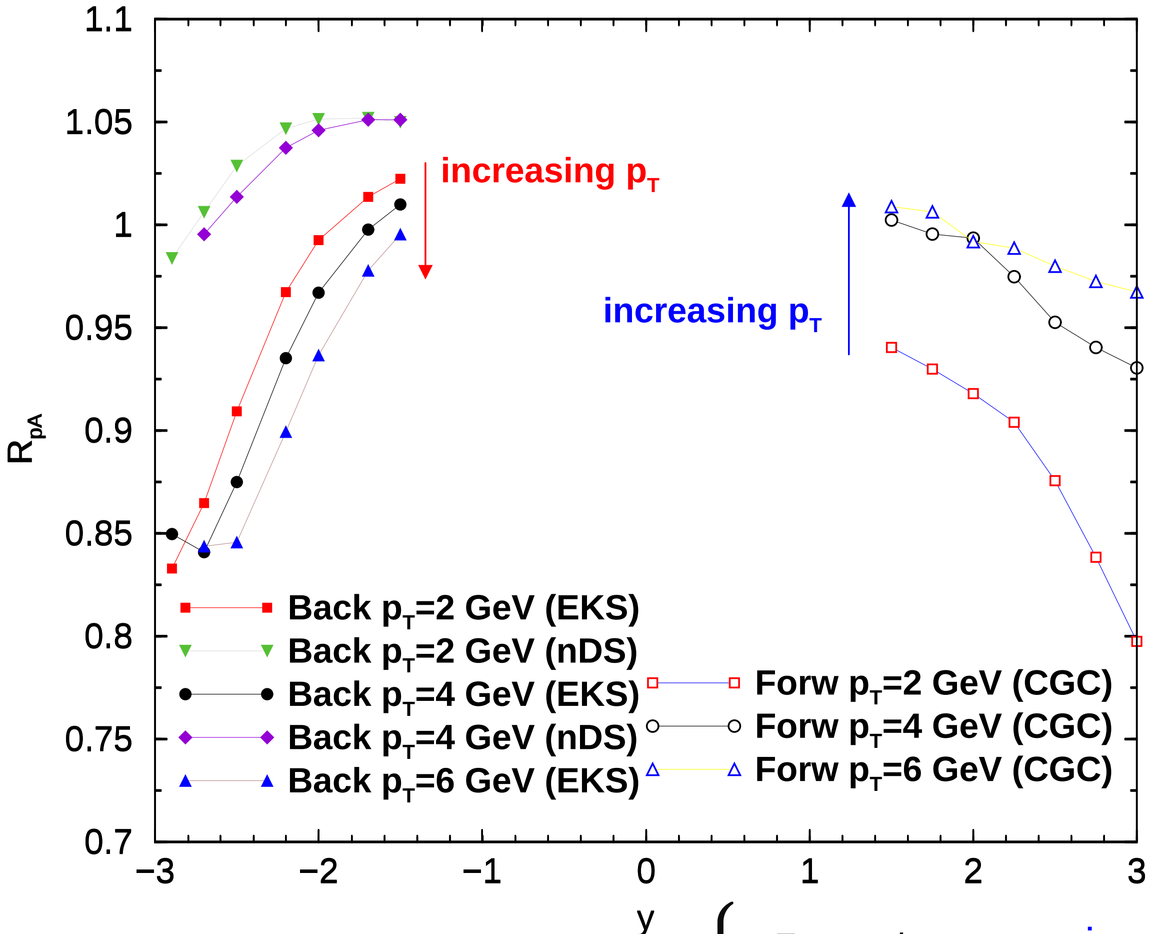

- $R_{pA} \Rightarrow p_T$ behavior.

$\left\{ \begin{array}{l} \text{Forward} \Rightarrow\ p_T \text{ increases} \Rightarrow R_{pA} \text{ enlarged (saturation)} \\ \text{Backward} \Rightarrow\ p_T \text{ increases} \Rightarrow R_{pA} \text{ reduced (large } x \text{ effects)} \end{array} \right.$

M.A. Betemps, MBGD, E.G. de Oliveira, hep-ph/0607247.

Cronin at backward-forward rapidities

- Hadrons

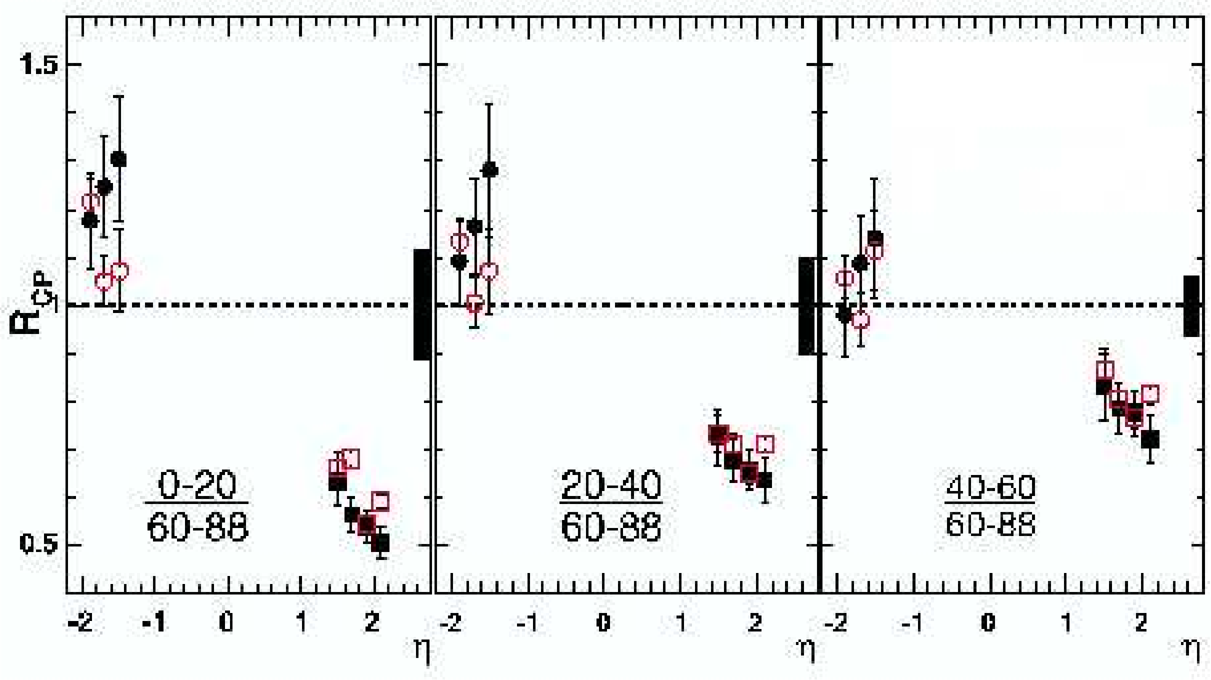

- Pronounced peak at backward rapidities (0.5 GeV <p_T< 4 GeV).
- R_{pA} for dileptons prediction for RHIC does not present such a peak.
- Cronin peak at backward rapidities at RHIC energies $\Rightarrow$ large x effects + final state effect.

S.S. Adler, et al. PHENIX *Collaboration, Phys. Rev. Lett.* **94***, 082302 (2005).*

Dilepton $\times$ Hadrons

R_{pA}	Forward	Backward
Dileptons	- Suppression of Cronin peak. - Saturation	**Rapidity Spectra** - Weak enhancement of R_{pA} in comparison with forward. - (RHIC) - Large x nuclear effects. - (LHC) - Large and small x nuclear effects. **Transverse Momentum** (RHIC) - R_{pA} reduces as p_T increases (large x effects) (LHC) - two behaviors (small and large x effects)
Hadrons	- Suppression of Cronin peak. - Saturation - Initial state effect.	- Enhanced Cronin peak in the rapidity spectra in comparison with forward (DATA). - Large x nuclear effects + final state effects (Dileptons indicate that).

Conclusions

- Saturation effects should be present at RHIC, hadrons and dileptons, at forward rapidities.
- Nuclear modification ratio suppression at forward rapidities for dileptons indicates the Cronin suppression for hadrons as initial state effect.
- At backward rapidities dileptons present different p_T dependence at RHIC (large x nuclear effects) comparing with the forward ones (saturation) (non symmetric).
- At LHC energies and backward rapidities, the p_T distribution for the ratio R_{pA} present distinct behaviors comparing very backward (large x effects) and more central rapidities (shadowing).
- Cronin effect peak in the rapidity spectra for hadrons at backward rapidities should be due to $\Rightarrow$ final state effects + large x nuclear effects.